Electronic Supplementary Material (ESI)

A dual-template strategy to engineer hierarchically porous Fe-N-C electrocatalyst for high-performance cathode of Zn-air batteries

Dan Wang, [a] Hao Xu, [a] Peixia Yang,*[a] Lihui Xiao, [a] Lei Du,*[a] Xiangyu Lu, [a] Ruopeng Li, [a] Jinqiu Zhang, [a] and Maozhong An [a]

a MIIT Key Laboratory of Critical Materials Technology for New Energy Conversion and Storage, School of Chemistry and Chemical Engineering, Harbin Institute of Technology, Harbin, 150001 China.

*E-mail: yangpeixia@hit.edu.cn, lei.du@hit.edu.cn

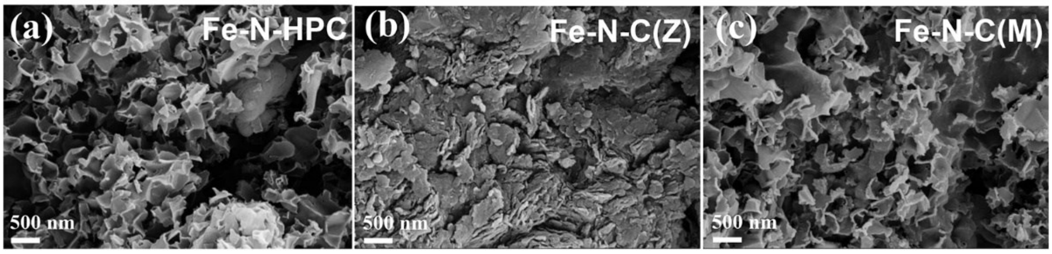

Fig. S1 SEM images of (a) Fe-N-HPC, (b) Fe-N-C(Z) and (c) Fe-N-C(M).

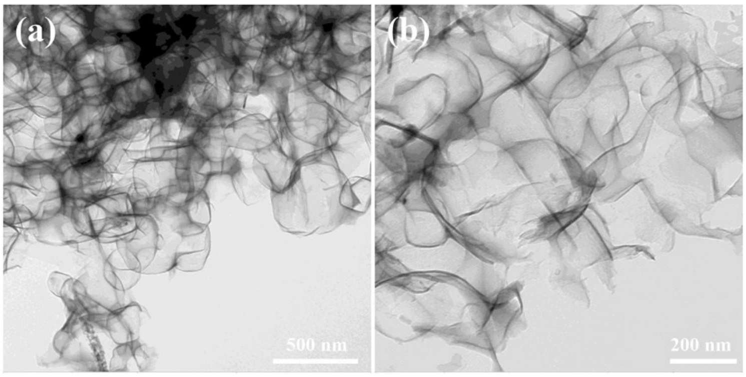

Fig. S2 TEM images of Fe-N-C(M).

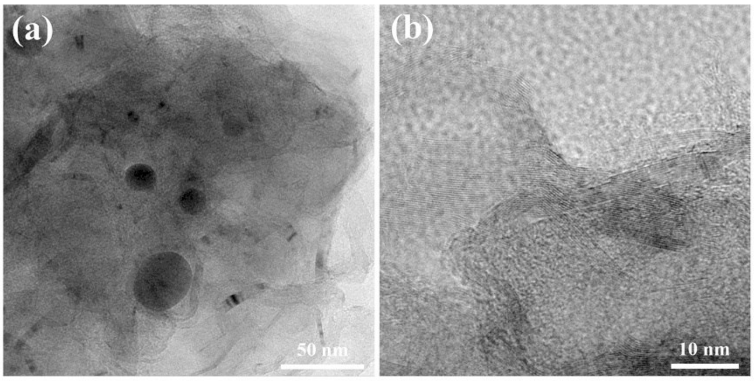

Fig. S3 (a) TEM and (b) HRTEM images of Fe-N-C(Z).

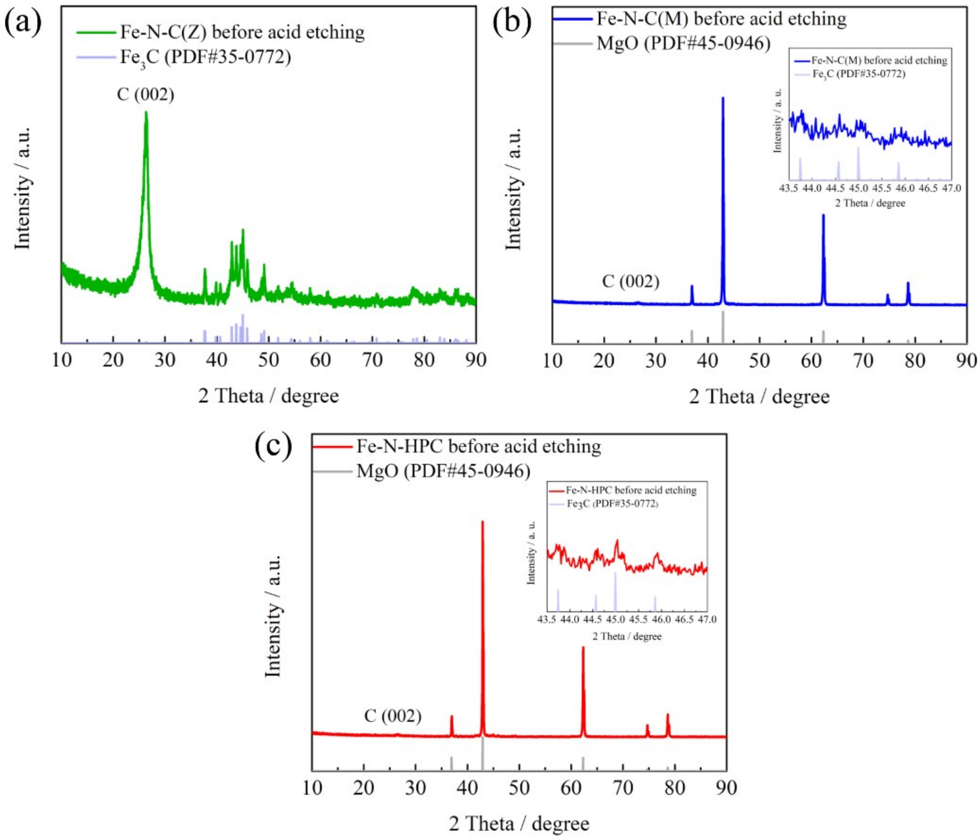

Fig. S4 The XRD patterns of (a) Fe-N-C(Z), (b) Fe-N-C(M) and (c) Fe-N-HPC before acid etching.

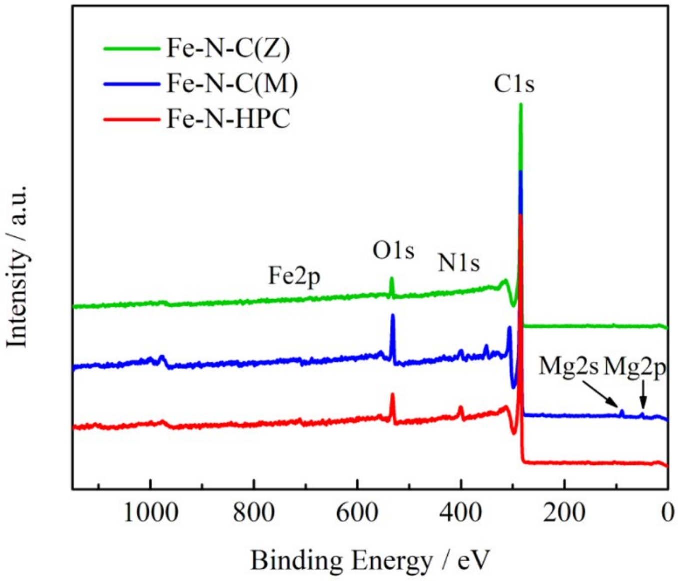

Fig. S5 XPS survey spectrum of Fe-N-C(Z), Fe-N-C(M) and Fe-N-HPC.

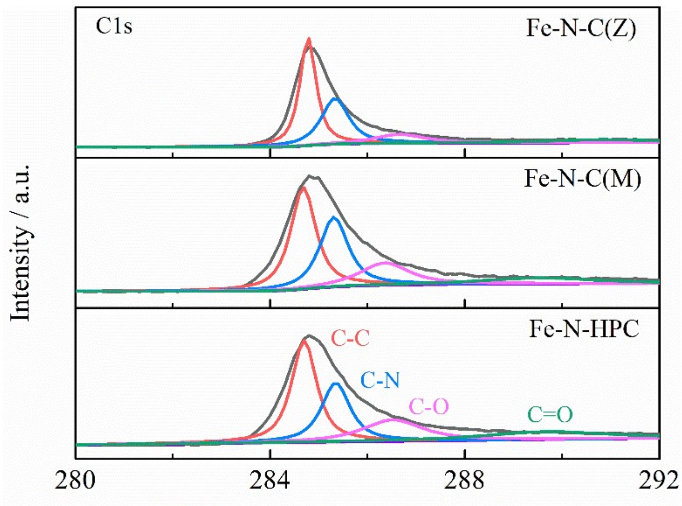

Fig. S6 High-resolution C1s XPS spectra of Fe-N-C(Z), Fe-N-C(M) and Fe-N-HPC.

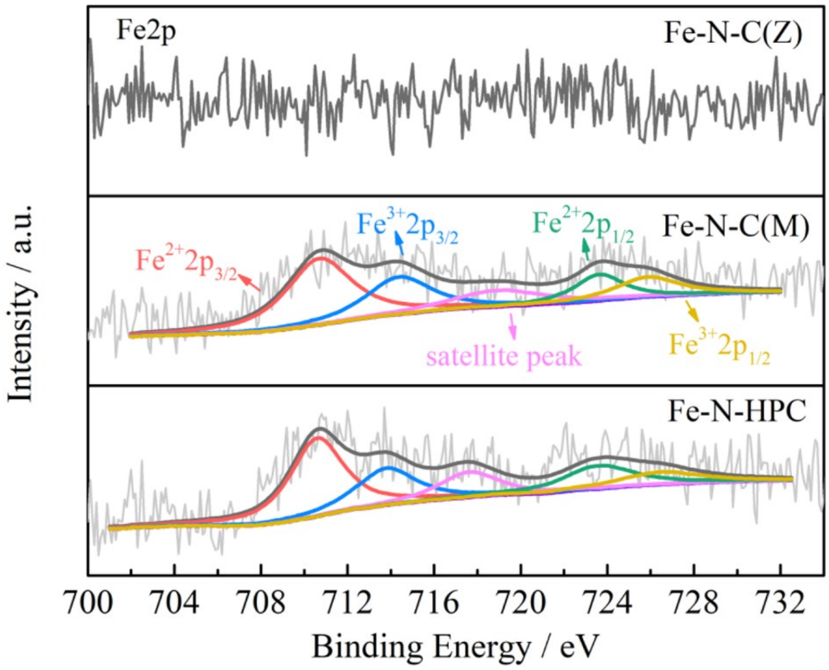

Fig. S7 High-resolution Fe2p XPS spectra of Fe-N-C(Z), Fe-N-C(M) and Fe-N-HPC.

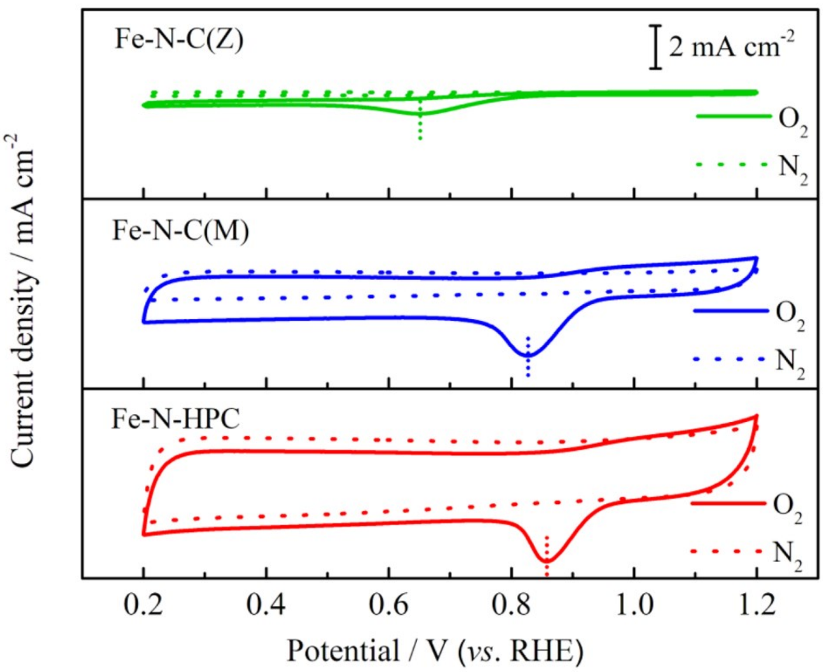

Fig. S8 CV curves of Fe-N-C(Z), Fe-N-C(M) and Fe-N-HPC in O_2-saturated and N_2-saturated 0.1 M KOH solution, respectively.

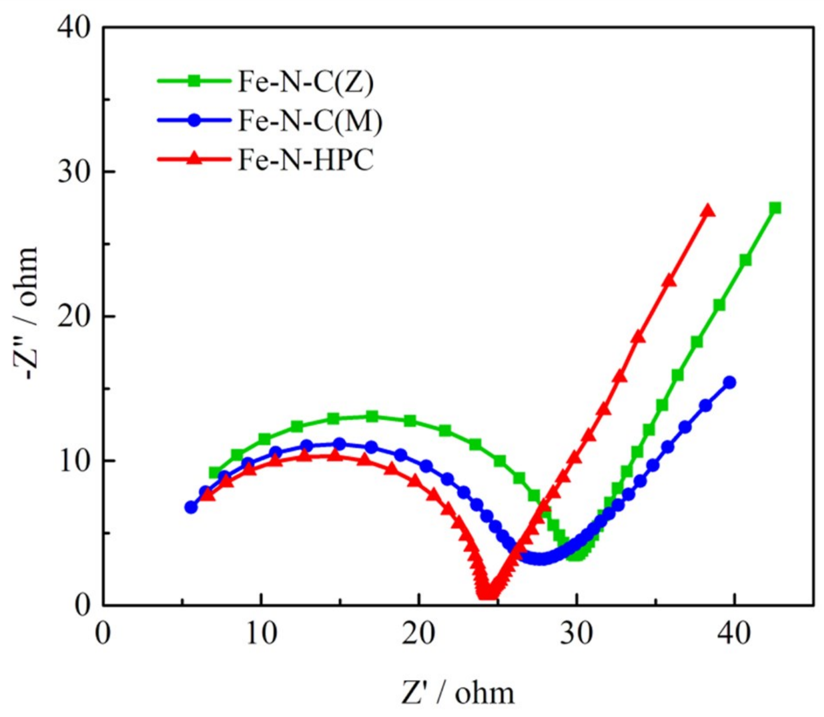

Fig. S9 Electrochemical impedance spectroscopy (EIS) of Fe-N-C(Z), Fe-N-C(M) and Fe-N-HPC in 0.1 M KOH.

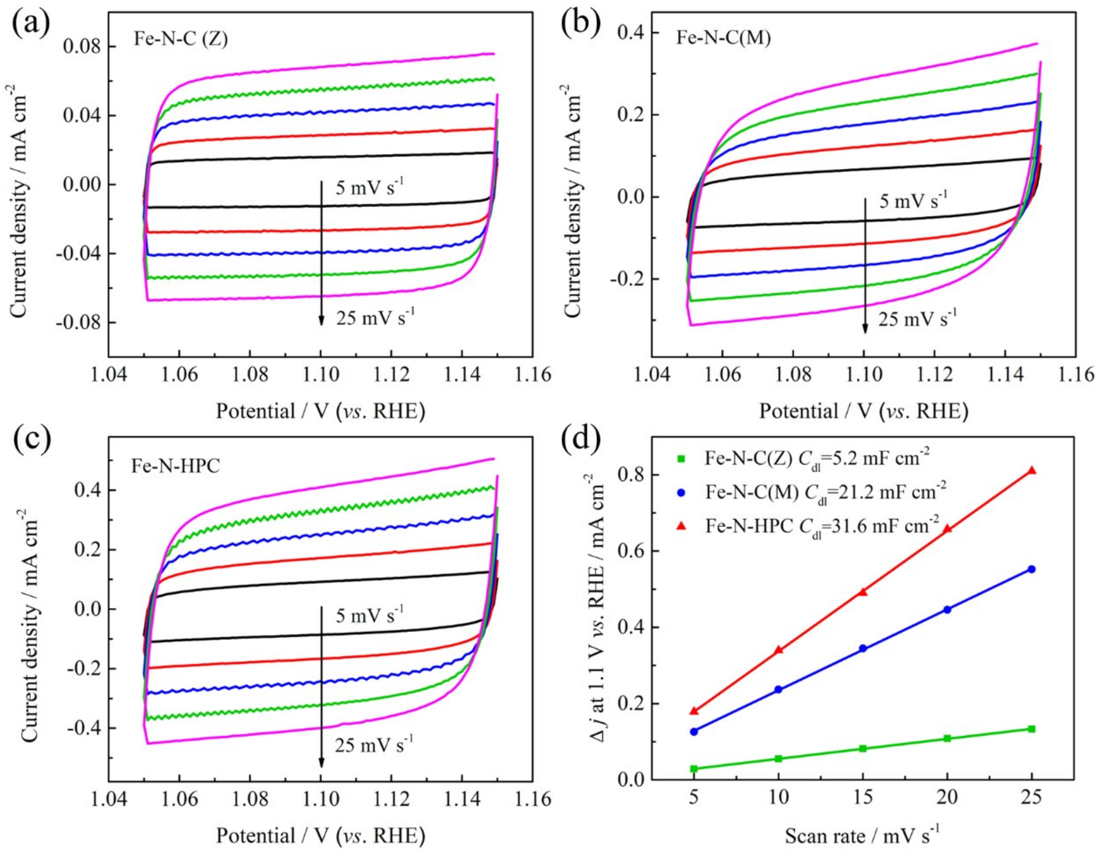

Fig. S10 CV curves of (a) Fe-N-C(Z), (b) Fe-N-C(M) and (c) Fe-N-HPC, respectively, at various scan rates (5 mV/s, 10 mV/s, 15 mV/s, 20 mV/s and 25 mV/s). (d) Plots of the extraction of the C_{dl} from CV curves at various scan rates.

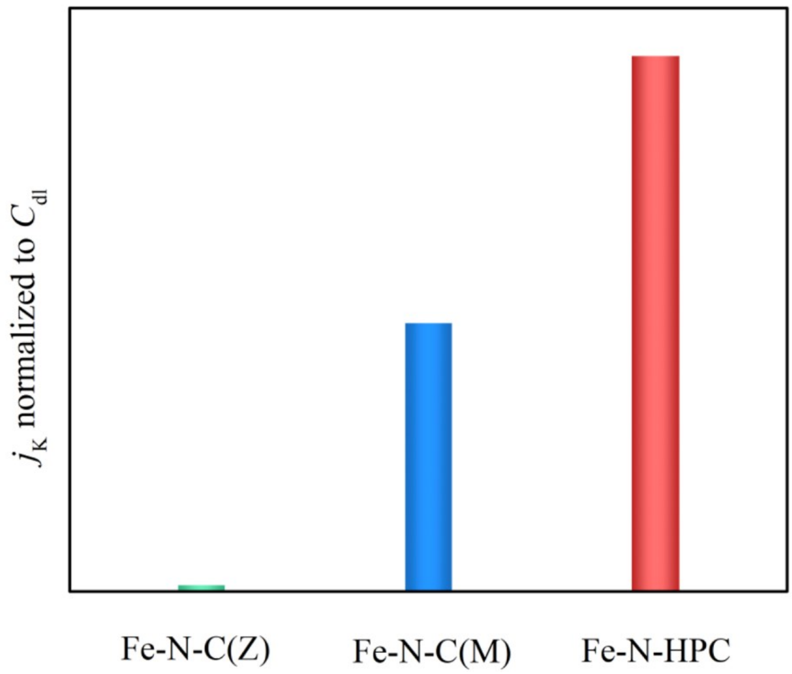

Fig. S11 The j_K@0.90 V with respect to C_{dl} for Fe-N-C(Z), Fe-N-C(M) and Fe-N-HPC in 0.1 M KOH.

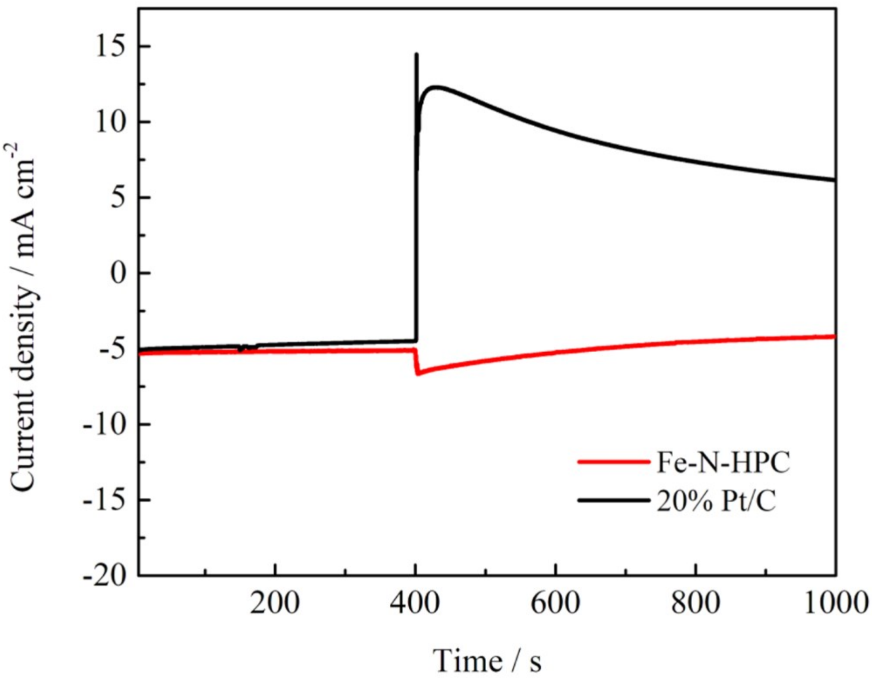

Fig. S12 Chronoamperometric responses of Fe-N-HPC and 20% Pt/C at 0.75 V in O_2-sarurated 0.1 M KOH followed by adding methanol.

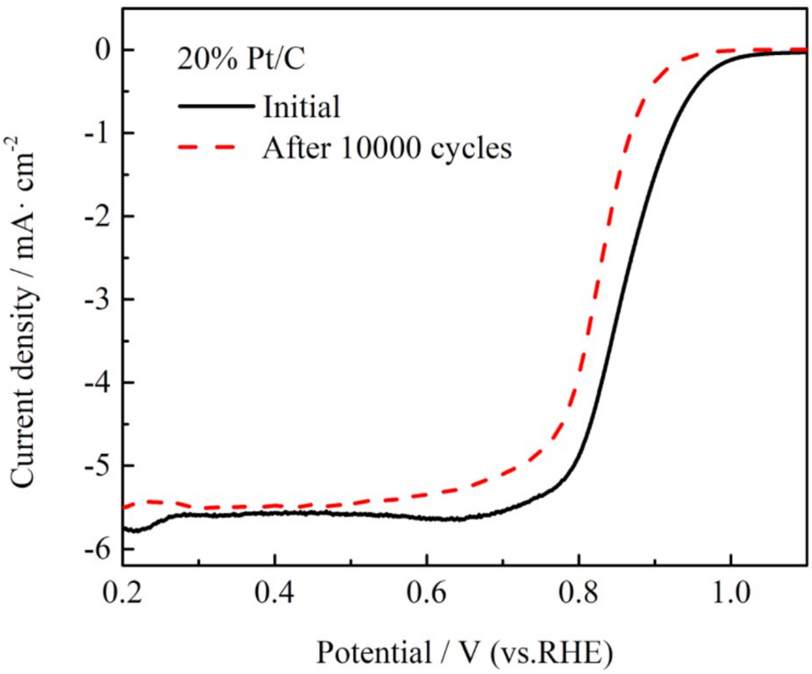

Fig. S13 ORR polarization curves of 20% Pt/C before and after 10 000 potential cycles in alkaline media.

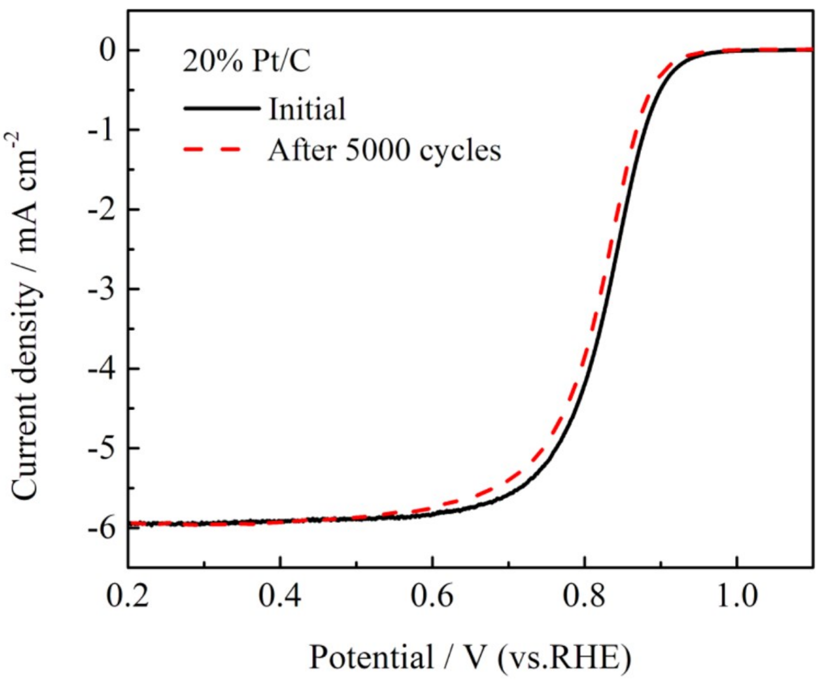

Fig. S14 ORR polarization curves of 20% Pt/C before and after 5 000 potential cycles in acidic media.

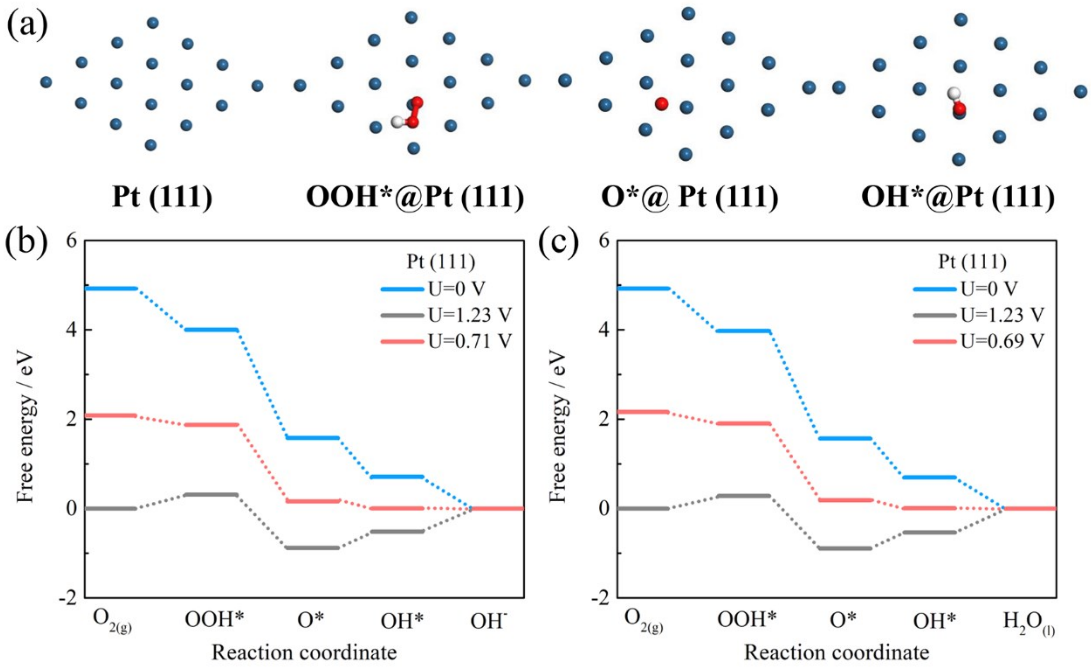

Fig. S15 (a) Structure of Pt(111) plane and the adsorption configurations of the ORR intermediates on the surface of Pt(111) plane where dark cyan, red, and white balls represent platinum, oxygen, and hydrogen atoms, respectively; * denotes the adsorption state. Free energy diagrams of ORR on Pt(111) plane in (b) alkaline and (c) acidic media.

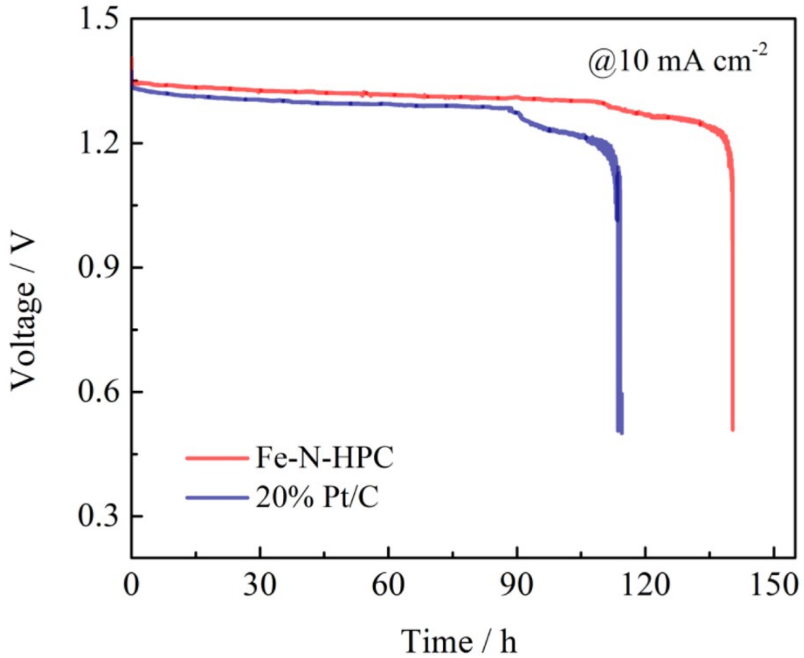

Fig. S16 Galvanostatic discharge curves at 10 mA cm^{-2} of Zn-air batteries employing Fe-N-HPC and Pt/C as the cathode catalysts.

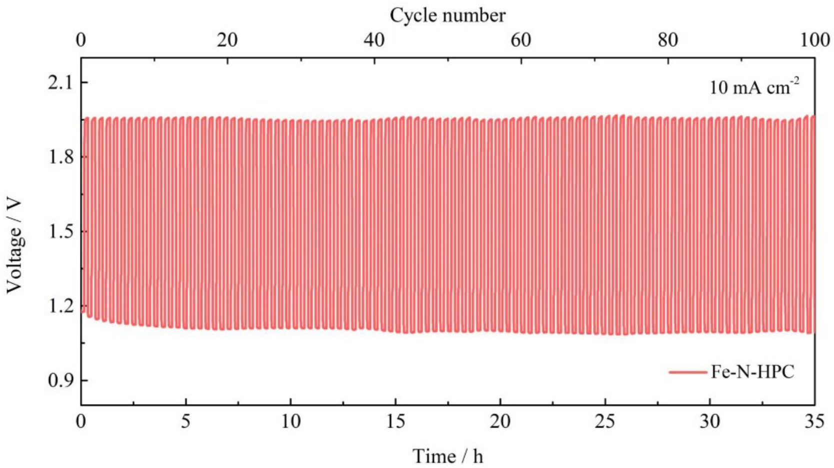

Fig. S17 Charge/discharge curves of the Zn-air battery using Fe-N-HPC catalyst at a current density of 10 mA cm^{-2} (20 min per cycle).

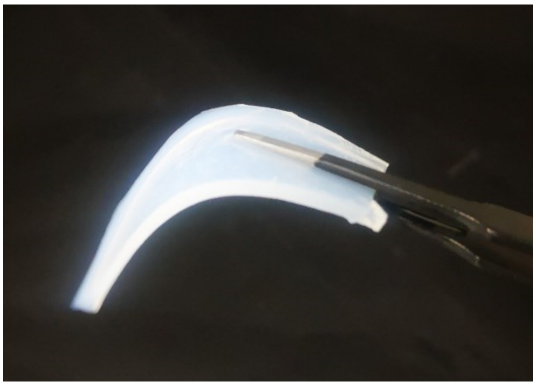

Fig. S18 A digital image of the as-prepared flexible PVA gel film.

Table S1. The content of C, N, O and Fe of the prepared catalysts obtained from XPS.

	Atomic Concentration %				Mass Concentration %			
	C	N	O	Fe	C	N	O	Fe
Fe-N-C(Z)	94.97	1.10	3.89	0.04	93.47	1.26	5.10	0.17
Fe-N-C(M)	87.90	2.88	8.64	0.59	83.32	3.18	10.9	2.59
Fe-N-HPC	90.23	3.93	5.23	0.61	86.26	4.38	6.66	2.70

Table S2. The content of different types of N (%) for the prepared catalysts obtained from XPS.

Sample	Pyridinic N	Fe-N	Pyrrolic N	Graphitic N	Oxidized N
Fe-N-C(Z)	16.2	14.3	22.5	25.8	21.2
Fe-N-C(M)	13.8	14.7	21.5	33.9	16.1
Fe-N-HPC	18.7	18.0	16.4	30.3	16.6

Table S3. A comparison table of the ORR performance between this work and recently reported Fe-N-C catalysts in alkaline and acidic media.

Materials	$E_{1/2}$ (V) (*vs.* RHE) in 0.1 M KOH	$E_{1/2}$ (V) (*vs.* RHE) in 0.1 M $HClO_4$ or 0.5 M H_2SO_4	References
Fe-N-HPC	0.910	0.800 ($HClO_4$)	This work
Fe-N-C	0.82	0.54 ($HClO_4$)	J. Mater. Chem. A, 2017, 5, 3336-3345.
Fe_3C/NG-800	0.86	0.77 ($HClO_4$)	Adv. Mater., 2015, 27, 2521-2527.
SA-Fe-NHPC	0.93	0.76 ($HClO_4$)	Adv. Mater. 2020, 1907399
Fe-N/C-700	0.84	0.672 ($HClO_4$)	Small, 2016, 12, 5710-5719.
Fe-Phen-N-800	0.86	0.71 ($HClO_4$)	J. Mater. Chem. A, 2016, 4, 19037-19044.
Fe-N-CNT/PC	0.88	0.79 ($HClO_4$)	J. Am. Chem. Soc., 2016, 138, 15046-15056
FePhen@MOF-ArNH3	0.86	0.79 ($HClO_4$)	Nat. Commun., 2015, 6, 7343.
Fe SA/NPCs	0.83	0.77 (H_2SO_4)	Appl. Catal. B Environ., 2020, 278, 119270

SA-Fe-N-1.5-800	0.910	0.812 (H_2SO_4)	Adv. Energy Mater. 2018, 1801226
Fe-N/MPC2	0.88	0.70 (H_2SO_4)	Appl. Catal. B Environ., 2017, 205, 637-653.

Table S4. A summary of the performance of liquid and all-solid-state Zn-air batteries with M-N-C cathode catalysts.

Materials	Liquid Zn-air batteries			All-solid-state Zn-air batteries	References
	Peak power density (mW cm^{-2})	Specific capacity (mAh·g_{Zn}^{-1})	Energy density (Wh kg_{Zn}^{-1})	Peak power density (mW cm^{-2})	
Fe-N-HPC	164.8	735.2	952.8	116.8	This work
Fe-N-C/N-OMC	113	711	—	—	Appl. Catal. B Environ., 2021, 280, 119411
FeCo-N-C-700	150	518	—	—	J. Mater. Chem. A, 2020, 8, 9355-9363
NGM-Co	152	750	840	~28	Adv. Mater. 2017, 29, 1703185
Fe-N-C-(PANI+CM+g-C_3N_4)	120	686	—	—	J. Mater. Chem. A, 2020, 8, 7273
SilkNC/KB	91.2	614.7	727.6	32.3	Chem. Mater. 2019, 31, 1023-1029

Fe@C-NG/NCNTs	101.3	682.6	764.5	—	J. Mater. Chem. A, 2018, 6, 516-526
FeNC-1000	55	680	—	—	ACS Appl. Mater. Interfaces 2018, 10, 10778-10785